Tightening the Hydrophobic Belt: Effects of Backbone and Donor Group Variation on Podand Ligand Complexes of the Lanthanides

Mark P. Lowe, P. Caravan, Steven J. Rettig, and Chris Orvig*

Department of Chemistry, University of British Columbia, 2036 Main Mall, Vancouver, BC, Canada V6T 1Z1

Received November 25, 1997

The N_4O_3 tripodal aminomethylene phosphinato ligand tris(4-phenylphosphinato-3-methyl-3-azabutyl)amine (H_3ppma) forms mono- and bis(ligand) complexes with lanthanide(III) metal ions Ln when Ln = Sm−Lu. The formation constants of the Lu ($\log \beta_1 = 1.79$, $\log \beta_2 = 4.40$) and the Yb ($\log \beta_1 = 2.25$, $\log \beta_2 = 4.42$) complexes were determined at pH = 1.5 using an unusual ^{31}P NMR spectroscopic method. The molecular structure of the lutetium complex $[Lu(H_3ppma)_2](NO_3)_3 \cdot 3H_2O$ ($C_{60}H_{96}LuN_{11}O_{24}P_6$) was solved by X-ray methods; it crystallizes in the trigonal space group $R\bar{3}c$, with $a = 19.060(1)$ Å, $c = 36.395(3)$ Å, and $Z = 6$. The structure was solved by Patterson methods and was refined by full-matrix least-squares procedures to $R = 0.024$ ($R_w = 0.025$) for 2061 reflections with $I > 3(I)$. The ligand coordinates in a tridentate manner through the three phosphinate oxygens, resulting in a bicapped octahedral structure of exact S_6 symmetry, which is preserved in solution as shown by ^{1}H and ^{31}P NMR spectroscopies (CD_3OD, DMSO-d_6). The two N_3O_3 tripodal amine phenol ligands 1,1,1-tris(((2-hydroxy-5-sulfobenzyl)amino)methyl)ethane (H_6tams) and 1,2,3-tris((2-hydroxy-5-sulfobenzyl)amino)-propane (H_6taps) showed a binding modality different from that with H_3ppma, forming N_3O_3 encapsulated complexes whereby all six donor atoms bind to the lanthanide. This complexation was investigated potentiometrically at 25 °C and 0.16 M NaCl. log *K* values of $[M(tams)]^{3-}$ ($[M(Htams)]^{2-}$) for M: La, 9.17; Nd, 11.19; Gd, 11.86 (18.41); Ho, 12.71 (19.40); Yb, 13.78 (20.11). log *K* values of $[M(taps)]^{3-}$ ($[M(Htaps)]^{2-}$) for M: La, 11.33 (18.47); Nd, 13.59 (20.13); Gd, 14.50 (20.88); Ho, 14.71 (21.15); Yb, 15.15 (21.54). The formation constants show an increasing affinity for the heavier lanthanides, with H_6taps forming the more stable complexes. ^{17}O NMR spectroscopy of $[Dy(tams)]^{3-}$ and $[Dy(taps)]^{3-}$ indicated the presence of three inner-sphere water molecules, implying a 9-coordinate Dy in each complex. The factors governing the coordination geometries in the solid and solution states and chelation of these and related metal ion complexes are discussed with reference to the hydrophobic belt.

Introduction

The vigorous pursuit of suitable chelating agents for trivalent metal ions such as the group 13 metals and the lanthanides is a result of their deleterious effects (e.g., concern over aluminum neurotoxicity[1]) and their burgeoning use in vivo as diagnostic probes, such as the use of gallium and indium radionuclides[2] in radiopharmaceuticals or the exploitation of the physical properties of the lanthanides[3] as luminescent, EPR, and NMR shift probes as well as their widespread application as magnetic resonance imaging contrast agents.[4] Similarities in oxophilicity (e.g., Al(III) and Ln(III)) and ionic radii (e.g., In(III) and Ln(III)) do not necessarily result in a complementary chemistry for the respective group 13 and lanthanide ions. Recent work[5] in our group has focused on the chelation of both the aforementioned metal ions with a variety of mixed nitrogen/oxygen donors in amine phenol tripodal ligands; however, until the water-soluble sulfonated analogues were synthesized,[6,7] little was known of the solution behavior in water. The coordination mode of the ligand can be metal dependent. For instance, in aqueous solution, H_6trns (see Chart 1) forms bicapped bis(ligand) lanthanide complexes in which bonding is solely through the phenolic oxygens,[7] whereas Ga(III) and In(III) form

* To whom correspondence should be addressed. Fax: 604-822-2847. Tel: 604-822-4449. E-mail: orvig@chem.ubc.ca.

(1) Perl, D. P. *Environ. Health Perspect.* **1985**, *63*, 149. (b) Crapper-McLachlan, D. R. *Neurobiol. Aging* **1986**, *7*, 525. (c) Liss, L. *Aluminum Neurotoxicity*; Pathotox Publishers: Park Forest, IL, 1980.
(2) Welch, M. J.; Moerlein, S. M. In *Inorganic Chemistry in Biology and Medicine*; Martell, A. E., Ed.; American Chemical Society: Washington, DC, 1980; p 121. (b) Green, M. A.; Welch, M. J. *Nucl. Med. Biol.* **1989**, *16*, 435. (c) Zhang, Z.; Lyster, D. M.; Webb, G. A.; Orvig, C. *Nucl. Med. Biol.* **1992**, *19*, 327.
(3) Martin, R. B.; Richardson, F. S. *Q. Rev. Biophys.* **1979**, *12*, 181. (b) Meares, C. F.; Wensel, T. G. *Acc. Chem. Res.* **1984**, *17*, 202. (c) *Lanthanide Probes in Life, Chemical, and Earth Sciences*; Bünzli, J.-C. G., Choppin, G. R., Eds.; Elsevier: Amsterdam, 1989. (d) Bünzli, J.-C. G. *Inorg. Chim. Acta* **1987**, *139*, 219. (e) Horrocks, W. DeW., Jr.; Albin, M. *Prog. Inorg. Chem.* **1984**, *31*, 1. (f) Gupta, R. K.; Gupta, P. *J. Magn. Reson.* **1982**, *47*, 344. (g) Pike, M. M.; Springer, C. S. *J. Magn. Reson.* **1982**, *46*, 348. (h) Sherry, A. D.; Geraldes, C. F. G. C.; Cacheris, W. P. *Inorg. Chim. Acta* **1987**, *139*, 137.
(4) Lauffer, R. B. *Chem. Rev.* **1987**, *87*, 901.
(5) Liu, S.; Wong, E.; Karunaratne, V.; Rettig, S. J.; Orvig, C. *Inorg. Chem.* **1993**, *32*, 1756. (b) Liu, S.; Wong, E.; Rettig, S. J.; Orvig, C. *Inorg. Chem.* **1993**, *32*, 4268. (c) Liu, S.; Rettig, S. J.; Orvig, C. *Inorg. Chem.* **1992**, *31*, 5400. (d) Liu, S.; Gelmini, L.; Rettig, S. J.; Thompson, R. C.; Orvig, C. *J. Am. Chem. Soc.* **1992**, *114*, 6081. (e) Liu, S.; Yang, L.-W.; Rettig, S. J.; Orvig, C. *Inorg. Chem.* **1993**, *32*, 2773. (f) Berg, D. J.; Rettig, S. J.; Orvig, C. *J. Am. Chem. Soc.* **1991**, *113*, 2528. (g) Smith, A.; Rettig, S. J.; Orvig, C. *Inorg. Chem.* **1988**, *27*, 3929. (h) Caravan, P.; Rettig, S. J.; Orvig, C. *Inorg. Chem.* **1997**, *36*, 1306. (i) Caravan, P.; Mehrkhodavandi, P.; Orvig, C. *Inorg. Chem.* **1997**, *36*, 1316.
(6) Caravan, P.; Orvig, C. *Inorg. Chem.* **1997**, *36*, 236.
(7) Caravan, P.; Hedlund, T.; Liu, S.; Sjöberg, S.; Orvig, C. *J. Am. Chem. Soc.* **1995**, *117*, 11230.

S0020-1669(97)01488-2 CCC: $15.00
Published on Web 03/19/1998

Chart 1

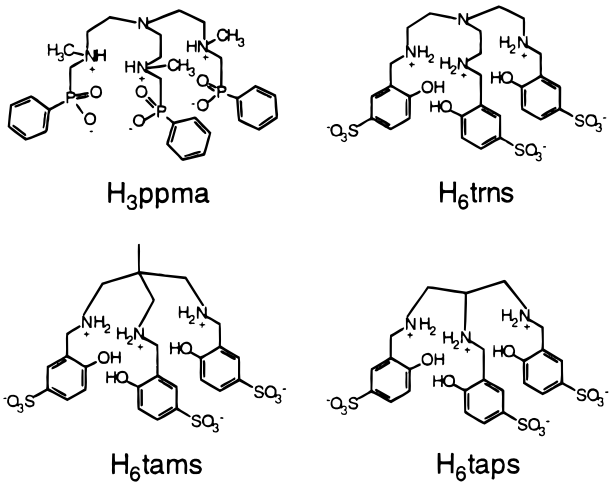

1:1 encapsulated complexes in which bonding occurs with both oxygen and nitrogen donors, while Al(III) does not form a stable complex with H_6trns in aqueous solution. The capped and bicapped lanthanide complexes of H_6trns have 16-membered chelate rings, much larger than the five- and six-membered rings in the encapsulated complexes. It has been suggested[7] that there is an effect which predisposes the ligand to a binding posture, for example the inter- and intrastrand hydrogen bonding between protonated nitrogens and phenolic oxygens. The hydrogen bonding, coupled with the large chelate ring size, can result in a ligand which suffers little or no strain energy in accommodating differently sized lanthanide ions, and thus the changes in stability noted (an unprecedented 5 orders of magnitude increase in stability from Nd to Yb) correlated with the increasing effective nuclear charge.[7]

In an effort to gain some further insight into the aqueous chemistry of H_6trns with the lanthanides, the aqueous lanthanide coordination chemistry of two other smaller tripodal amine phenol ligands, H_6tams and H_6taps (see Chart 1), has been investigated herein. Should these ligands coordinate in a similar manner as H_3trns^{3-} (bicapped), 14- and 13-membered chelate rings would be formed upon lanthanide coordination. We were interested in the effect of the large chelate ring size on metal ion stability and selectivity. There has been no structural chemistry reported for either the Ln−tams or Ln−taps systems; however, as was seen with the group 13 metals,[6] variations in the number of potential donor atoms, the number of chelate rings formed upon coordination, and the size of the chelate rings formed (five- or six-membered rings) can have a profound effect upon metal ion selectivity and coordination geometry (Scheme 1). Instead, this change in backbone results in a dramatic change in binding modality in that H_6tams and H_6taps react with Ln(III) ions in the presence of base to form encapsulated complexes wherein all six donor atoms of the ligand (i.e., N_3O_3 coordination) coordinate to the lanthanide ion. This change in coordination mode relative to H_6trns (capped, bicapped) also produces a lower selectivity for heavy lanthanide chelation.

Changing the phenolic oxygen donor atoms of H_6trns to phosphinic acids, H_3ppma (see Chart 1), resulted in bicapped binding for the group 13 metals (Scheme 1).[8] The first stepwise equilibrium constant K_1 (formation of the monocapped species) is less than that of the second K_2 (formation of the bicapped species). This behavior was also noted in the lanthanide H_3trns^{3-} system. It was found that the difference between K_1 and K_2 increased as the metal ion size increased. In light of this size effect, we wished to further explore this phenomenon by using larger metal ions, i.e., the lanthanides. Reported here are the results of the reactions of Ln(III) with H_3ppma where, once more, bicapped species are formed.

The anomalous equilibrium constant behavior was also observed and is discussed in relation to the similar trend observed for H_6trns, whereby the anomaly can be described in terms of hydrophobic effects (see Discussion).

Experimental Section

Materials. Sodium deuterioxide (NaOD, 40%), deuterium chloride (DCl, 12 M), and the lanthanide atomic absorption standards were obtained from Aldrich. Hydrated lanthanide nitrates and chlorides were obtained from Alfa. Deuterium oxide (D_2O), methanol-d_4 (CD_3OD), and DMSO-d_6 were purchased from Cambridge Isotope Laboratories. All were used without further purification. Tris(4-phenylphosphinato-3-methyl-3-azabutyl)amine trihydrochloride monohydrate (H_3ppma·3HCl·H_2O),[8] 1,1,1-tris(((2-hydroxy-5-sulfobenzyl)amino)methyl)ethane dihemihydrate (H_6tams·2.5H_2O),[6] and 1,2,3-tris((2-hydroxy-5-sulfobenzyl)amino)propane dihemihydrate (H_6taps·2.5H_2O)[6] were prepared as described in earlier papers.

Instruments. ^{1}H NMR spectra (200 and 300 MHz) were referenced to DSS or TMS and recorded on Bruker AC-200E and Varian XL 300 spectrometers. ^{13}C NMR (75.5 MHz, referenced to DSS or TMS), ^{31}P NMR (121.0 MHz, referenced to external 85% H_3PO_4), natural-abundance ^{17}O NMR (40.7 MHz, referenced to H_2O), and ^{139}La NMR (42.4 MHz, referenced to 0.1 M La(ClO_4) in 1 M $HClO_4$) spectra were recorded on the latter instrument. Mass spectra were obtained on a Kratos Concept II H32Q (Cs^+, LSIMS) instrument with thioglycerol or 3-nitrobenzyl alcohol as the matrix. Infrared spectra were obtained as KBr disks in the range 4000−400 cm^{-1} on a Galaxy Series 5000 FTIR spectrometer. Analyses for C, H, and N were performed by Mr. Peter Borda in this department.

Synthesis of the Lanthanide−H_3ppma Complexes. The preparation of the lutetium complex (as the trihydrate) is representative for the lanthanides Er−Lu, and the preparation of the terbium complex (as the pentahydrate) is representative for the lanthanides Sm−Ho, Yb, and Lu (in the case of Sm, Eu, and Ho, the metal chloride was used). All the complexes prepared with their elemental analyses and NMR data are listed in Tables 1 and 2 (mass spectral and infrared data are in the Supporting Information).

[Lu(H_3ppma)$_2$][NO_3]$_3$·3H_2O. The pH of an aqueous solution (4 mL) of H_3ppma·3HCl·H_2O (0.200 g, 0.257 mmol) and Lu(NO_3)$_3$·6H_2O (0.060 g, 0.128 mmol) was raised to 2.0 using 3 M NaOH. Colorless prisms deposited after 2 h; these prisms were filtered off and dried under vacuum to yield 0.145 g (66%). Yields for the other complexes: Yb, 78%; Tm, 50%; Er, 53%.

[Tb(H_3ppma)$_2$][NO_3]$_3$·5H_2O. An aqueous solution (0.7 mL) of H_3ppma·3HCl·H_2O (0.100 g, 0.128 mmol) was added to Tb(NO_3)$_3$·5H_2O (0.057 g, 0.128 mmol) in 0.7 mL of H_2O. Colorless hexagonal crystals deposited after 24 h; these were filtered off and dried under vacuum to yield 0.064 g (58%). Yields for the other complexes: Lu, 71%; Yb, 73%; Ho, 43%; Dy, 50%; Gd, 63%; Eu, 40%; Sm, 48%.

NMR Measurements. The variable-pH ^{1}H NMR spectra of the H_6tams and H_6taps complexes were run in D_2O with the pD values being measured by a Fisher Accumet 950 pH meter employing an Accumet Ag/AgCl combination microelectrode. The pD values were converted to pH by adding 0.40 to the observed reading.[9] The ^{17}O NMR experiments with Dy(III) were recorded at 21 °C, with a spectral window of 1000 Hz, a 90° pulse width of 18 μs, and an acquisition time of 0.256 s; this gave 512 data points. Two thousand transients were collected per spectrum. The ^{17}O line widths for H_2O were about 60 Hz. Concentrations employed ranged from 1 to 40 mM. The dysprosium-induced shifts (DIS) were obtained from the observed shift by making a correction for the bulk magnetic susceptibility of the

(8) Lowe, M. P.; Rettig, S. J.; Orvig, C. *J. Am. Chem. Soc.* **1996**, *118*, 10446.

(9) Glasoe, P. K.; Long, F. A. *J. Phys. Chem.* **1960**, *64*, 188.

Scheme 1

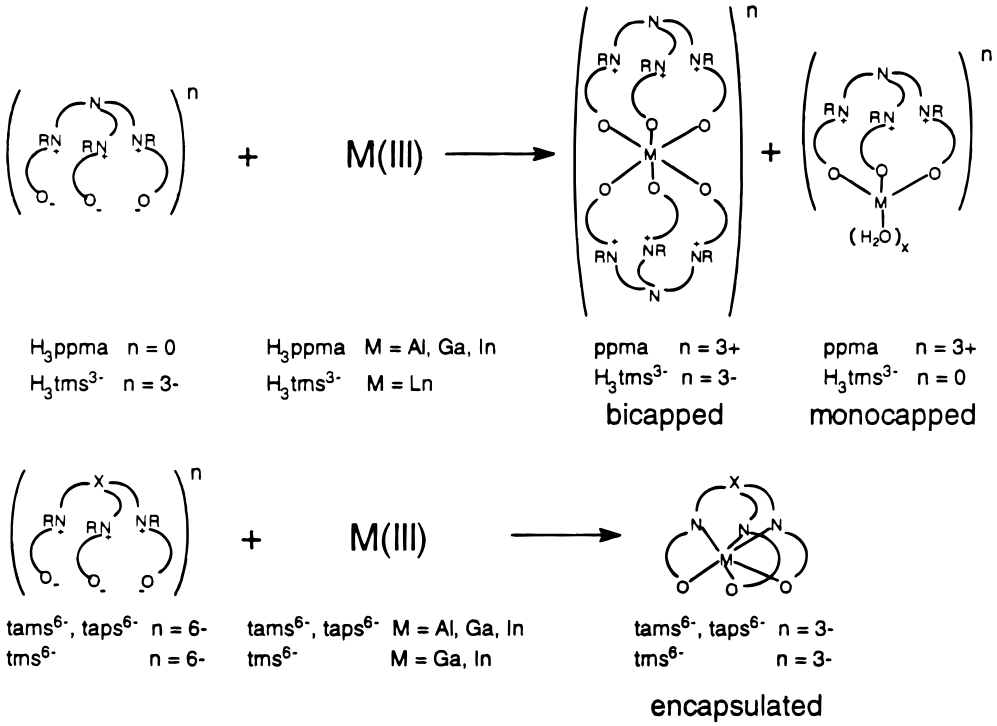

Table 1. $[Ln(H_3ppma)_2](X)_3 \cdot YH_2O$ (X = NO_3, Cl) Complexes Prepared in This Study and Their Elemental Analyses

	% C		% H		% N	
formula	calc	found	calc	found	calc	found
$C_{60}H_{90}LuN_{11}O_{21}P_6 \cdot 3H_2O$	41.99	41.88	5.64	5.87	8.98	8.95
$C_{60}H_{90}LuN_{11}O_{21}P_6 \cdot 5H_2O$	41.13	41.26	5.75	5.65	8.79	8.55
$C_{60}H_{90}N_{11}O_{21}P_6Yb \cdot 3H_2O$	42.04	42.34	5.64	5.60	8.99	8.91
$C_{60}H_{90}N_{11}O_{21}P_6Yb \cdot 5H_2O$	41.17	41.19	5.76	5.62	8.80	8.68
$C_{60}H_{90}N_{11}O_{21}P_6Tm \cdot 3H_2O$	42.14	42.24	5.66	5.61	9.01	8.79
$C_{60}ErH_{90}N_{11}O_{21}P_6 \cdot 3H_2O$	42.18	41.88	5.66	5.87	9.02	8.95
$C_{60}Cl_3H_{90}HoN_8O_{12}P_6 \cdot 5H_2O \cdot 2HCl$	41.52	42.06	5.92	6.15	6.46	6.24
$C_{60}DyH_{90}N_{11}O_{21}P_6 \cdot 5H_2O$	41.42	41.66	5.79	6.04	8.86	8.50
$C_{60}H_{90}N_{11}O_{21}P_6Tb \cdot 5H_2O$	41.51	41.23	5.81	5.85	8.87	8.59
$C_{60}GdH_{90}N_{11}O_{21}P_6 \cdot 5H_2O$	41.55	41.61	5.81	5.63	8.88	8.53
$C_{60}Cl_3EuH_{90}N_8O_{12}P_6 \cdot 5H_2O \cdot 2HCl$	41.84	41.99	5.97	6.10	6.50	6.25
$C_{60}Cl_3H_{90}N_8O_{12}P_6Sm \cdot 5H_2O \cdot 2HCl$	41.87	42.13	5.97	6.14	6.51	6.38

Table 2. ^1H and ^{31}P NMR Chemical Shifts[a] for $[Ln(H_3ppma)_2](NO_3) \cdot 3H_2O$ in CD_3OD (Ln = Er−Lu)

	$[Tm(H_3ppma)_2]^{3+}$	$[Er(H_3ppma)_2]^{3+}$	$[Yb(H_3ppma)_2]^{3+}$	$[Lu(H_3ppma)_2]^{3+}$
H_A	−17.04	−5.97	−0.27	3.24
$H_{A'}$	−13.06	−3.93	0.44	2.37
H_B	−22.92	−7.91	−0.63	4.74
$H_{B'}$	−26.94	−8.69	−0.76	3.00
H_C	−4.24	−0.02	1.88	3.03
H_D	−3.80	−1.93	2.14	2.30
$H_{D'}$	9.39	5.00	3.19	3.00
H_F	45.08	23.25	13.59	7.50
H_G	19.69	12.23	9.22	7.46
H_H	17.07	11.2	8.83	7.34
P	14.61	−6.86	34.41	15.29

[a] For labeling see Figure 6. NMR spectra were referenced to TMS in CD_3OD and chemical shifts were corrected for bulk magnetic susceptibilty.

solution.[10] Stock solutions were prepared from metal nitrates in D_2O (H_2O), and the metal−ligand solutions were prepared by pipetting required amounts of stock solution and adjusting the pH with acid or base. In the equilibrium measurements, the ionic strength was controlled by addition of NaCl.

For the Ln−H_3ppma (Ln = Yb, Lu) equilibrium constant studies using $^{31}P\{H\}$ NMR, conditions as described in a previous publication were used.[8] Metal ion stock solutions (50 mM) were prepared from the hydrates of $Lu(NO_3)_3$ and $Yb(NO_3)_3$. All solutions contained a fixed amount of M^{3+} (25 mM) with the ligand concentration varied ($R = [L]_T/[M]_T$) as $0.25 < R < 4$. Solutions were made up to a volume of 0.8 mL, and the pH was adjusted to 1.5. The solutions were allowed to equilibrate for 48 h prior to collection of the spectra. The respective peak integrals enabled a quantitative measurement (long delay times of 1.6 s were employed) of free ligand ([L]). The knowledge of [L] allowed $\bar{n}$, the ratio of bound ligand to total metal, to be calculated ($\bar{n}$

(10) Bertini, I.; Luchinat, C. *NMR of Paramagnetic Molecules in Biological Systems*; Benjamin/Cummings: Menlo Park, CA, 1986; Vol. 3.

Table 3. Selected Crystallographic Data for $Lu[(H_3ppma)_2](NO_3)_3 \cdot 3H_2O$

empirical formula	$C_{60}H_{96}LuN_{11}O_{24}P_6$	ρ_{calc}, g/cm^3	1.493
fw	1716.29	T, °C	21
crystal system	trigonal	radiation	Cu
space group	$R\bar{3}c$	λ, Å	1.541 78
a, Å	19.060(1)	μ, cm^{-1}	43.66
c, Å	36.395(3)	transm factors	0.82−1.00
V, Å^3	11449(1)	R^a	0.024
Z	6	$R_w{}^b$	0.025

[a] $R = \sum||F_o| - |F_c||/\sum|F_o|$. [b] $R_w = [\sum w(|F_o| - |F_c|)^2/\sum w|F_o|^2]^{1/2}$.

$= ([L]_T - [L])/[M]_T$). A plot of $\bar{n}$ vs [L] resulted in a curve from which the variables β_1 and β_2 could be calculated using computer curve fitting software.

Potentiometric Equilibrium Measurements. The procedure was the same as detailed in a previous paper.[7] The measurements were made at 25.0 ± 0.1 °C and $\mu = 0.16$ M (NaCl). The pK_a values of the ligands were checked whenever a different synthetic batch of ligand was used, and fresh ligand solutions were always employed. (For H_6taps: pK_a(**1**) = 1.7, pK_a(**2**) = 6.54, pK_a(**3**) = 7.78, pK_a(**4**) = 8.73, pK_a(**5**) = 9.77, pK_a(**6**) = 11.24. For H_6tams: pK_a(**1**) = 2.92, pK_a(**2**) = 6.56, pK_a(**3**) = 7.95, pK_a(**4**) = 8.91, pK_a(**5**) = 9.81, pK_a(**6**) = 11.19.[6]) The lanthanide solutions were prepared by dilution of the appropriate atomic absorption standards. Since the lanthanides do not hydrolyze below pH 6, the excess acid in the solutions could be obtained by titrating with standard NaOH and analyzing for the strong acid by the method of Gran.[11]

The ratios of ligand to metal used were in the range 1:2 < L:M < 4:1, and concentrations were in the range 0.5−2.5 mM. A minimum of five titrations were performed for each metal. The metal−H_6taps and metal−H_6tams solutions were titrated to just beyond 6 equiv of NaOH/H_6taps (H_6tams), because of slow hydrolysis beyond this point. Although complexation was rapid (1−3 min per point to give a stable pH reading), care was taken to ensure that no trace hydrolysis or precipitation was occurring by monitoring up to 30 min for pH drift. The protonation constants for the lanthanide−ligand stability constants were determined by using the program BEST.[12] H_6tams and H_6taps both reacted with Ln(III) to coordinate as hexadentate ligands, liberating 6 equiv of acid per ligand. Typically 100 data points were collected with about 80−90% of the points being in the buffer region of metal−ligand complexation and the remaining points in the strong acid region being used as a check of excess acid concentration.

X-ray Crystallographic Analysis of $Lu(H_3ppma)_2](NO_3)_3 \cdot 3H_2O$ [$C_{60}H_{96}LuN_{11}O_{24}P_6$]. Selected crystallographic data appear in Table 3. The final unit-cell parameters were obtained by least-squares calculations on the setting angles for 25 reflections with $2\theta = 55.7-68.7°$. The intensities of three standard reflections, measured every 200 reflections throughout the data collection, decayed linearly by 2.7%. The data were processed[13] and corrected for Lorentz and polarization effects, decay, and absorption (empirical, based on azimuthal scans).

The structure of $[C_{60}H_{90}LuN_8O_{12}](NO_3)_3 \cdot 3H_2O$ was solved by the Patterson method. The structure analysis was initiated in the centrosymmetric space group $R\bar{3}c$ on the basis of the E-statistics, this choice being confirmed by subsequent calculations. The nitrate anions and water molecules were modeled as (1:1) disordered about a point of S_6 symmetry. Because of thermal motion and near overlap of disordered components, the nitrate groups deviate from ideal geometry. Refinement of the structure in the noncentrosymmetric space group $R3c$ failed to resolve the disorder. All non-hydrogen atoms were refined with anisotropic thermal parameters. Hydrogen atoms were fixed in calculated positions (N−H = 0.91 Å, C−H = 0.98 Å, $B_H = 1.2B_{bonded\ atom}$). A correction for secondary extinction (Zacharaisen type) was applied, the final value of the extinction coefficient being 1.73(3) × 10^{-7}. Neutral-atom scattering factors for all atoms and anomalous dispersion corrections for the non-hydrogen atoms were taken from refs 14 and 15, respectively. Selected bond lengths and bond angles appear in Table 4. Complete tables of crystallographic data, final atomic coordinates and equivalent isotropic thermal parameters, anisotropic thermal parameters, bond lengths, bond angles, torsion angles, intermolecular contacts, and least-squares planes are included as Supporting Information.

Table 4. Selected Bond Lengths (Å) and Angles (deg)[a] for $[Lu(H_3ppma)_2](NO_3)_3 \cdot 3H_2O$

Lengths			
Lu(1)−O(1)	2.190(2)	P(1)−O(1)	1.492(2)
P(1)−O(2)	1.487(2)	P(1)−C(4)	1.826(3)
P(1)−C(5)	1.786(3)	N(1)−C(1)	1.471(3)
N(2)−C(2)	1.518(3)	N(2)−C(3)	1.498(4)
N(2)−C(4)	1.506(3)		
Angles			
O(1)−Lu(1)−O(1)^a	88.72(6)	O(1)−Lu(1)−O(1)^b	180.0
O(1)−Lu(1)−O(1)^c	91.28(6)	O(1)−P(1)−O(2)	119.1(1)
O(1)−P(1)−C(4)	103.5(1)	O(1)−P(1)−C(5)	108.41(10)
O(2)−P(1)−C(4)	109.8(1)	O(2)−P(1)−C(5)	111.3(1)
C(4)−P(1)−C(5)	103.5(1)	Lu(1)−O(1)−P(1)	145.2(1)
C(1)−N(1)−C(1)^a	108.7(2)	C(2)−N(2)−C(3)	111.5(2)
C(2)−N(2)−C(4)	110.2(2)	C(3)−N(2)−C(4)	110.7(2)
N(1)−C(1)−C(2)	113.4(2)	N(2)−C(2)−C(1)	113.1(2)
P(1)−C(4)−N(2)	112.6(2)	P(1)−C(5)−C(6)	121.8(2)
P(1)−C(5)−C(10)	119.5(2)		

[a] Symmetry operations: (*a*) $-y, x-y, z$; (*b*) $-x, -y, 1-z$; (*c*) $y, -x+y, 1-z$.

Results

$[Ln(H_3ppma)_2]^{3+}$ (Ln = Lu−Sm). The synthesis of the bis(ligand) complexes as hydrated salts was achieved by mixing stoichiometric (L:M = 2:1) amounts of aqueous solutions of metal nitrate or chloride and H_3ppma (with Er−Lu the pH was raised to 1.5). Precipitation of the resulting complexes occurred within a few hours to days, depending on the metal ion. The lanthanide complexes fall into two categories: The complexes of the smaller, heavier lanthanides (Er−Lu) were prepared in the same manner as their group 13 metal analogues[8] yielding cubic crystals, which analyzed as trihydrates. The complexes of the lighter lanthanides (Sm−Ho, and Yb and Lu for comparison) were prepared in a similar manner; however, no pH adjustment was made. Hexagonal plates were obtained; these analyzed as pentahydrates (and when a starting material metal chloride was used, two additional hydrochlorides were found). It is expected that this additional hydration is due to a different crystal lattice formed at lower pH; however the thin plates proved unsuitable for X-ray analysis. The IR spectra of the Er−Lu complexes resembled their group 13 analogues, with one of the three P−O stretches shifted to lower wavenumber as the metal ion increased in size, a trend which persisted through the lanthanide series from samarium to lutetium (ν_{PO} = 1154−1165 cm^{-1}). The P−O stretch at the highest wavenumber for the trihydrates, when Ln = Er−Lu (ν_{PO} = 1194−1190 cm^{-1}), changed for the pentahydrates of the earlier lanthanides Ln = Sm−Ho, Yb, and Lu (ν_{PO} = 1183−1180 cm^{-1}) likely due to a slight change in structure ($\cdot 3H_2O$ vs $\cdot 5H_2O$). It is unclear whether this is attributable to differences in hydrogen bonding or to a different coordination number; however, a large shift in the ν_{NH} stretch ($\Delta\nu_{NH} \approx 300$ cm^{-1}) along with a change of ν_{PO} indicated a change in hydrogen-bonding strength. The LSIMS (+) mass spectra showed

(11) Gran, G. *Acta Chem. Scand.* **1950**, *4*, 559.
(12) Motekaitis, R. J.; Martell, A. E. *Can. J. Chem.* **1982**, *60*, 2403.
(13) *teXsan*: *Crystal Structure Analysis Package*; Molecular Structure Corp.: The Woodlands, TX, 1985 and 1992.
(14) *International Tables for X-ray Crystallography*; Kynoch Press: Birmingham, England, 1974; Vol. IV, pp 99−102.
(15) *International Tables for Crystallography*; Kluwer Academic Publishers: Boston, MA, 1992; Vol. C, pp 200−206.

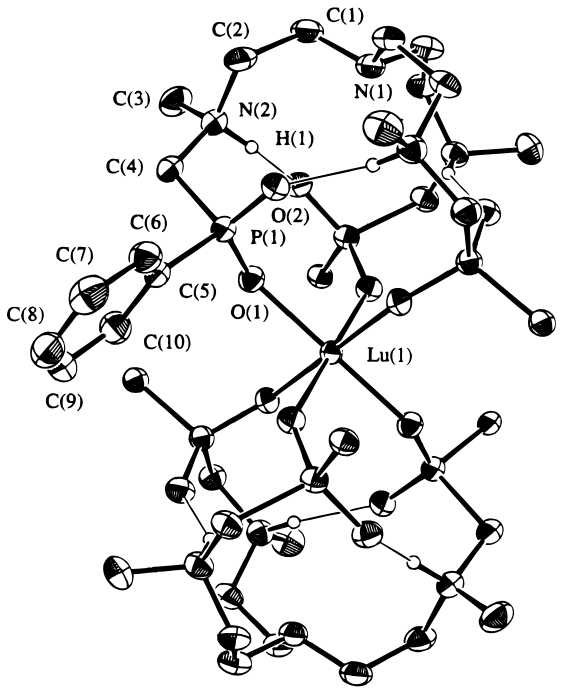

Figure 1. ORTEP representation of the cation in $[Lu(H_3ppma)_2]$-$(NO_3)_3 \cdot 3H_2O$ (25% probability thermal ellipsoids). Only one phenyl group is shown for clarity.

molecular ions $[ML_2-2H]^+$ and $[ML_2 - H]^{2+}$ at the appropriate *m*/*z* value for the bicapped species and ions for the monoligand species $[ML - 2H]^+$ and for the free ligand $[L + H]^+$ at $m/z = 651$.

X-ray Crystal Structure of $[Lu(H_3ppma)_2][NO_3]_3 \cdot 3H_2O$. Colorless prisms crystallized in the space group $R\bar{3}c$. An ORTEP representation of the $[Lu(H_3ppma)_2]^{3+}$ cation is shown in Figure 1, and selected bond distances and angles are listed in Table 4. The structure is that of a bicapped ML_2 complex, similar to that observed for the bis(ligand) tren-based amine phenolate−lanthanide complexes,[5e] and is isostructural and isomorphous with the indium structure.[8] The complex cation has exact S_6 symmetry. The O−Lu−O trans angle is crystallographically imposed at 180.0°, and the cis O−Lu−O angles are 88.72(6) and 91.28(6)°, resulting in nearly perfect octahedral geometry, expected because the ionic radius[16] of Lu^{3+} (0.861 Å) is similar to that of In^{3+} (0.800 Å), i.e., the ideal size to accommodate two ligands in a bicapped manner. The Lu−O distances of 2.190(2) Å are in the expected range, although few six-coordinate lutetium structures have been reported. This distance is only slightly longer than the In−O distance (2.117(3) Å) in the indium structure,[8] again reflecting the similar sizes of the ions. On coordination to the metal ion, the phosphorus atoms are rendered chiral, with half of the bicapped structure possessing all-*R* chirality and the other half all-*S*; i.e., the cation is the *RRRSSS* diastereomer. This opposing *RRRSSS* chirality generates the 6-fold symmetry and is indeed necessary to accommodate the six bulky phenyl rings because, once the phosphinates coordinate, the phenyls completely engulf the coordination sphere. Highly ordered intramolecular hydrogen bonding is observed from the protonated nitrogen N(2) to the phosphinate oxygen O(2) on an adjacent arm, where H···O = 1.87 Å (N···O = 2.684(3) Å) and N−H···O = 147°.

Formation Constants. Figure 2 shows experimental titration curves for the lanthanides with H_6tams (top) and H_6taps (bottom)

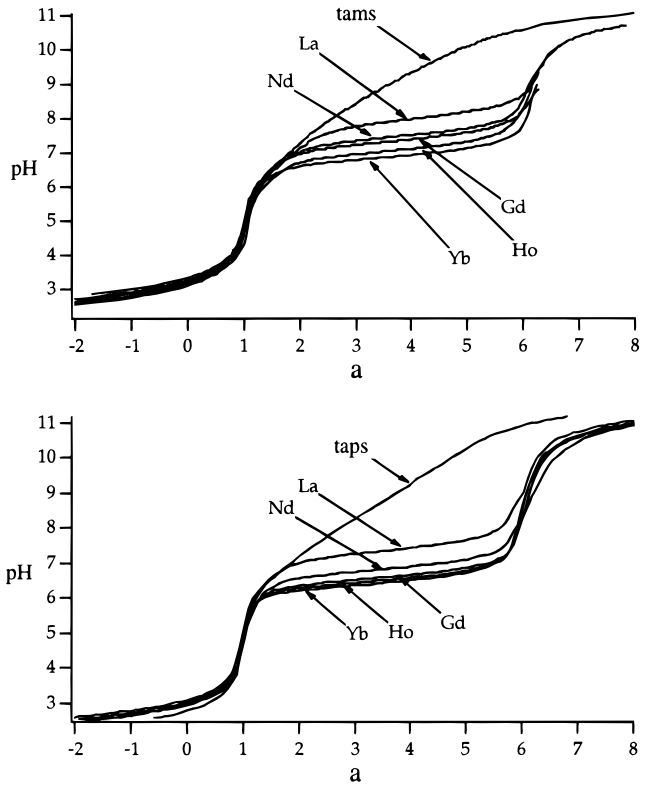

Figure 2. Experimental titration curves at 2 mM H_6tams−2 mM Ln(III) (top) and 2 mM H_6taps−2 mM Ln(III) (bottom) (*a* = moles of NaOH/moles of ligand).

at a ratio of 2 mM Ln(III):2 mM ligand. The equilibria in eqs 1 and 2 apply to these two systems (L = tams,[6−] taps[6−]). The

$$Ln^{3+} + L^{6-} \rightleftharpoons [Ln(L)]^{3-} \quad (1)$$

$$K_{Ln(L)} = [[Ln(L)]^{3-}]/[Ln^{3+}][L^{6-}]$$

$$Ln^{3+} + H^+ + L^{6-} \rightleftharpoons [Ln(HL)]^{2-} \quad (2)$$

$$K_{Ln(HL)} = [[Ln(HL)]^{3-}]/[Ln^{3+}][H^+][L^{6-}]$$

curves show plateaus which extend up to $a = 6$, indicating that the ligands are coordinating in a hexadentate fashion through all six N_3O_3 donor atoms; this is verified (and further emphasized) in the $\bar{n}$ plots (Figure 3) where the curves rise to $\bar{n} = 1$ and then plateau, even in the experiments with excess ligand. Analysis of the potentiometric data gave the stability constants listed in Table 5. It was necessary to include monoprotonated complexes in the model to improve the fit of the data, although these only form to a small extent (maximum ~ 25% of total Ln(III)). Both tams[6−] and taps[6−] are selective for the heavier lanthanides but much less so than is H_3trns[3−].[7]

Because of the very low pK_a's for H_3ppma,[8] formation constants for the ytterbium and lutetium complexes of H_3ppma were determined by a ^{31}P NMR approach highlighted previously.[8] ^{31}P NMR spectra were recorded for a series of solutions ($R = [L]_T/[M]_T$; L = H_3ppma; M = Yb, Lu) in the range $0.24 < R < 3.80$ (where [Lu] = [Yb] = 25 mM). A representative sample for the Yb study is shown in Figure 4. The resonance for free H_3ppma is clearly distinct from those for the metal complexes (ML and ML_2). Two resonances for both *RRRSSS* and *RRSSSR* diastereomers were noted, as was seen in the group 13 study.[8] It is much more difficult to assign these resonances as specific 1:1 and 2:1 species (cf. the case of the group 13

(16) Shannon, R. D. *Acta Crystallogr.* **1976**, *A32*, 751.

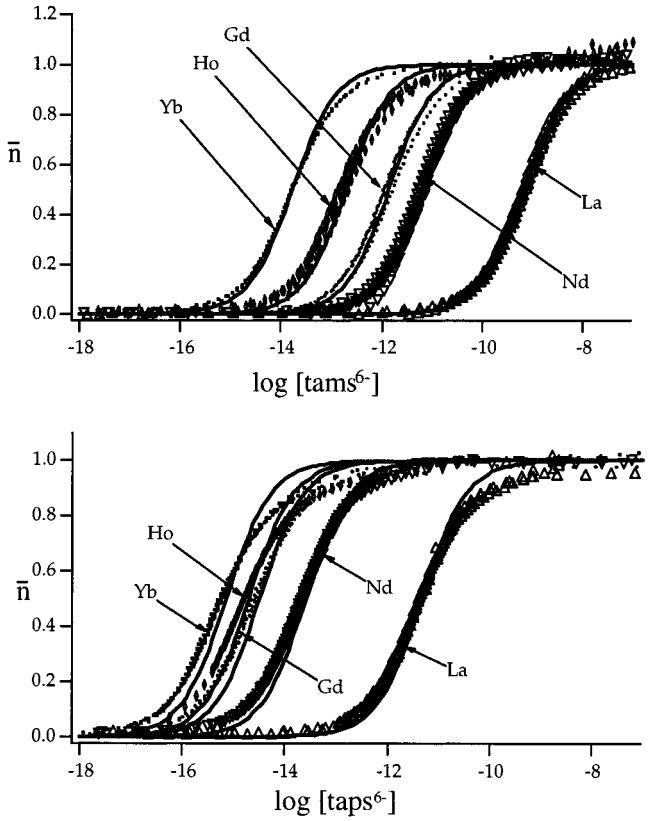

Figure 3. Experimental plots of $\bar{n}$ vs log [tams^{6-}] (top) and $\bar{n}$ vs log [taps^{6-}] (bottom). The solid lines were generated using the calculated stability constants, $K_{Ln(tams)}$ and $K_{Ln(taps)}$.

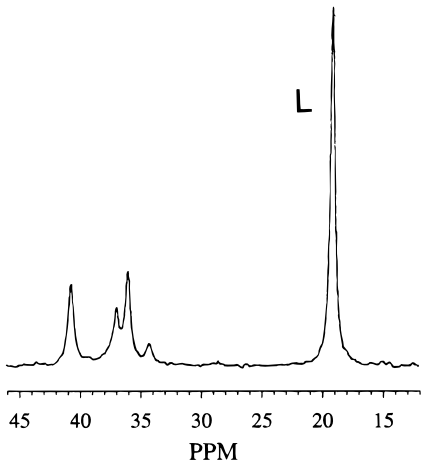

Figure 4. ^{31}P NMR spectrum (121.0 MHz) for the stability constant study of the Yb(III)−H_3ppma system. $R = [L]_T/[M]_T = 3.8$.

Table 5. Logarithms of the Formation Constants for Ln(III) with tams^{6-} and taps^{6-} (25 °C, $\mu = 0.16$ M (NaCl))

	tams^{6-}		taps^{6-}	
Ln(III)	[ML]/[M][L]	[HML]/[ML][H]	[ML]/[M][L]	[HML]/[ML][H]
La	9.17 (1)		11.33 (3)	7.14 (2)
Nd	11.19 (6)		13.59 (3)	6.54 (3)
Gd	11.86 (9)	6.55 (9)	14.50 (1)	6.38 (4)
Ho	12.71 (10)	6.69 (4)	14.71 (4)	6.44 (9)
Yb	13.78 (1)	6.33 (3)	15.15 (3)	6.39 (4)

metals where the additional tool of the metal NMR was invaluable); however the concentration of free ligand [L] is readily obtained from the integrals. From this value, $\bar{n}$ can be calculated for each experiment (see Experimental Section and ref 8). Assuming the formation of the 1:1 and 2:1 complexes

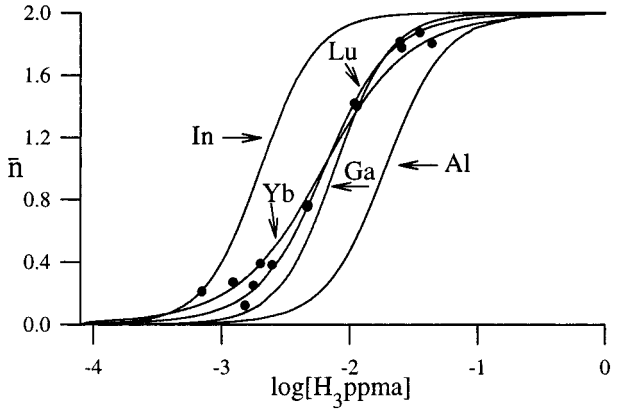

Figure 5. Plot of $\bar{n}$ vs [H_3ppma] for the Yb(III) (○) and Lu(III) (□) systems. (Solid lines indicate fits; symbols indicate experimental data.) The calculated curves for the group 13 metal ions[8] are included for comparison.

(eqs 3 and 4) where M = Yb, Lu and L = H_3ppma and using mass balance equations, $\bar{n}$ (the ratio of bound ligand to total metal) can be expressed as eq 5 in terms of the formation

$$M + L \rightleftharpoons ML \quad (3)$$

$$ML + L \rightleftharpoons ML_2 \quad (4)$$

$$\bar{n} = (\beta_1[L] + 2\beta_2[L]^2)/(1 + \beta_1[L] + \beta_2[L]^2) \quad (5)$$

constants β_1 and β_2 and free ligand [L]. From a plot of $\bar{n}$ vs [L], values of the formation constants obtained for Lu are log $\beta_1 = 1.79(7)$ and log $\beta_2 = 4.40(2)$ and for Yb are log $\beta_1 = 2.25(7)$ and log $\beta_2 = 4.42(5)$. A plot of $\bar{n}$ vs log [L] for Lu and Yb (also included are the data[8] for Al, Ga, and In) is shown in Figure 5. The curves rise to $\bar{n} = 2$ and then plateau, indicating formation of a 2:1 species.

Multinuclear NMR (^{1}H, ^{13}C, ^{31}P, ^{139}La). Solution NMR studies on the Ln(III)−H_6tams and Ln(III)−H_6taps systems were unrevealing. The ^{1}H NMR and ^{13}C NMR spectra of [Lu(taps)]$^{3-}$ in D_2O at pD 9 showed a series of broad overlapping resonances characteristic of fluxional behavior. The ^{1}H NMR spectra of [Lu(tams)]$^{3-}$, [La(tams)]$^{3-}$, and [La(taps)]$^{3-}$ were similar to those of the free ligand, suggesting fast exchange. A ^{139}La NMR study of 30 mM La(III)−30 mM H_6taps as a function of pH showed only one resonance at 0 ppm, the chemical shift of La_{aq}^{3+}. The line width of this resonance increased with pH, suggesting that [La(taps)]$^{3-}$ is in exchange with La_{aq}^{3+}.

The ^{1}H NMR spectra of the [Ln(H_3ppma)$_2$]$^{3+}$ complexes in CD_3OD where Ln = Er−Lu, all exhibit 10 resonances, corresponding to the 10 hydrogens labeled in Figure 6, the spectrum of the thulium complex. The observance of only 10 resonances clearly indicates the persistence of the S_6 symmetry in solution for all these H_3ppma complexes. The spectrum of the diamagnetic lutetium complex greatly resembles those obtained for the same structure with the group 13 metals[8] and is most similar to that of the indium complex, consistent with the similar ionic radii of the two metals. The resonances can be readily assigned from their coupling patterns (Lu), from their 2D ^{1}H−^{1}H COSY spectra, and from comparison with the group 13 metal complexes of H_3ppma. With the paramagnetic lanthanide (Er−Yb) complexes, dramatic chemical shifts are noted, with well-resolved and narrow resonances. The ^{31}P NMR spectra of these four late lanthanide complexes also exhibit S_6 symmetry in solution, showing a single narrow resonance for all six equivalent phosphorus atoms.

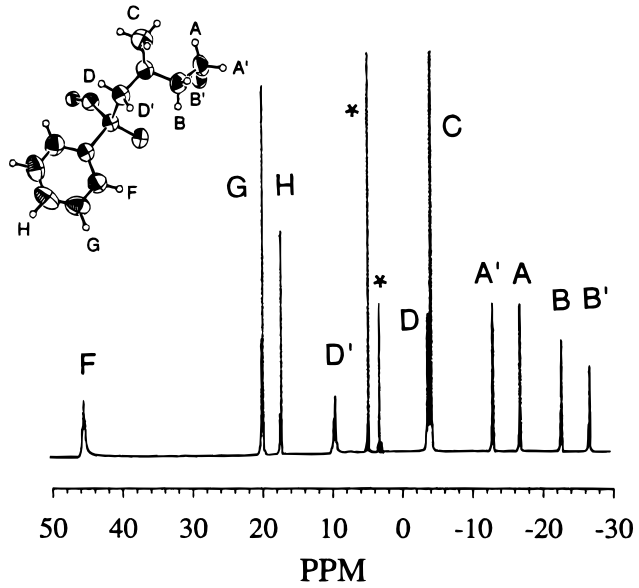

Figure 6. ^{1}H NMR spectrum (300.0 MHz) of $[Tm(H_3ppma)_2](NO_3)_3$ in CD_3OD (corrected for $\Delta\chi$, the shift due to the bulk magnetic susceptibility; $*$ = solvent).

On moving to the larger lighter lanthanides (Sm−Ho), a dramatic change in the respective ^{1}H/^{31}P NMR spectra is noted. The ^{31}P NMR spectra no longer indicate a single species in solution (four resonances are usually observed), resulting in a proliferation of resonances in the corresponding ^{1}H NMR spectra. The chemical shifts of the ^{31}P NMR resonances suggest that only complexes are present (i.e., no resonance for free H_3-ppma is evident), and thus one must assume that the solvent CD_3OD is interacting with the bicapped complex, forcing changes in geometry and/or stoichiometry. Even from these complex spectra, the 10 resonances corresponding to the *RRRSSS* diastereomer can usually be discerned when the lanthanide in question causes sufficient chemical shift separation (Tb−Ho). If a different solvent is used, i.e., DMSO-d_6, a dramatic simplification of the spectrum is observed. Ten resonances (broader than in CD_3OD) of the *RRRSSS* diastereomer are observed in the ^{1}H NMR spectrum, along with the spectrum of H_3ppma. This is reciprocated in the ^{31}P NMR spectrum where two resonances are seen, one of which is present in the CD_3OD spectrum and the other of which is a new one for free H_3ppma. Interestingly, if the Yb and Lu complexes are prepared in the same manner as those of Sm−Ho, i.e., no pH adjustment, as hexagonal crystals (analyzing as the pentahydrate), their respective NMR spectra are the same as those obtained by raising the pH (as the trihydrate); i.e., no decomposition or rearrangement is noted, which suggests the lanthanide is sufficiently small and/or tightly bound to prevent solvent interaction with metal ion.

The shift, Δ, induced at a nucleus of a ligand binding to a Ln(III) cation can be expressed as the sum of the diamagnetic shift (Δ_d), the contact shift (Δ_c), the pseudocontact shift (Δ_p), and the shift due to the bulk magnetic susceptibility (Δ_χ), eq 6.

$$\Delta = \Delta_d + \Delta_c + \Delta_p + \Delta_\chi \quad (6)$$

$$\Delta_\chi = 4\pi C(\mu_{eff}/2.84)^2/3T \quad (7)$$

The diamagnetic shift, which is usually relatively small, can be obtained from the shift of $[Lu(H_3ppma)_2]^{3+}$. Since the magnetic moments of the Ln(III) ions are relatively constant, the bulk magnetic susceptibility shift can be estimated from eq 7,[17] which applies to a superconducting solenoid, where C is the concentration (mM) of Ln(III), μ_{eff} is the effective magnetic moment for Ln(III), and T is the temperature (K). Calculated μ_{eff} values were taken from Figgis.[18] The contact and pseudocontact shifts can be expressed by eq 8,[17] where Δ_c and Δ_p are each expressed as the product of two terms.

$$\Delta' = \Delta - (\Delta_d + \Delta_\chi) = \Delta_c + \Delta_p = \langle S_Z\rangle F + C^D G \quad (8)$$

The first term ($\langle S_Z\rangle$ or C^D) is characteristic of the lanthanide but independent of the ligand, while the second term (F or G) is characteristic of the ligand in question but independent of the Ln(III) cation. Values for the lanthanide-dependent contact term, $\langle S_Z\rangle$, and pseudocontact term, C^D, have been calculated.[19−23] eq 8 can be separated into two linear forms, eqs 9 and 10.

$$\Delta'/C^D = F(\langle S_Z\rangle/C^D) + G \quad (9)$$

$$\Delta'/\langle S_Z\rangle = G(C^D/\langle S_Z\rangle) + F \quad (10)$$

Although both (9) and (10) are mathematically identical, Reilley et al.[24] have advocated the use of eq 9 when $F \gg G$ (and eq 10 when $G \gg F$) since the dependence on theoretical C^D (or $\langle S_Z\rangle$) will be minimized by a small intercept.

Figure 7 shows a plot of Δ'/C^D vs $\langle S_Z\rangle/C^D$ for the ^{1}H NMR spectra (top) and the ^{31}P NMR spectra (bottom) of $[Ln(H_3ppma)_2]^+$. For an isostructural series, a linear relationship is expected, whereby the parameters F and G may be obtained from slopes and intercepts of plots derived from eqs 9 and 10, respectively. This is clearly not observed in the structures presented in Figure 7. A difference between Er−Yb and Sm−Ho would be expected as analysis reveals additional water in the solid state; however a correlation for Er−Yb would certainly be assumed as all evidence points to an "isostructural miniseries". It is evident from these plots that there must be some change in ligand orientation.

^{17}O NMR. The natural-abundance ^{17}O NMR of water in the presence of a lanthanide ion and ligand gives a qualitative picture of complexation. Peters and co-workers have exploited the dysprosium-induced shift of water (DyIS) to estimate quantitatively the number of bound water molecules associated with various lanthanide complexes.[25−27] The DyIS of water was measured at varying dysprosium concentrations. The plot of DyIS versus [Dy(III)] was linear with a slope of −358 ppm/M. It had been previously established that the contact contribution in a paramagnetic Ln(III)-induced shift of a Ln(III)-bound ^{17}O nucleus is almost independent of the nature of the probed O-containing ligand in question and of other coligands coor-

(17) Peters, J. A.; Huskens, J.; Raber, D. J. *Prog. NMR Spectrosc.* **1996**, *28*, 283.
(18) Figgis, B. N. *Introduction to Ligand Fields*; Robert E. Krieger Publishing Co.: Malabar, FL, 1986.
(19) Golding, R. M.; Halton, M. P. *Aust. J. Chem.* **1972**, *25*, 2577.
(20) Pinkerton, A. A.; Rossier, M.; Spiliadis, S. *J. Magn. Reson.* **1985**, *64*, 420.
(21) Bleaney, B. *J. Magn. Reson.* **1972**, *8*, 91.
(22) Bleaney, B.; Dobson, C. M.; Levine, B. A.; Martin, R. B.; Williams, R. J. P.; Xavier, A. V. *J. Chem. Soc., Chem. Commun.* **1972**, 791.
(23) Golding, R. M.; Pyykkö, P. *Mol. Phys.* **1973**, *26*, 1389.
(24) Reilley, C. N.; Good, B. W.; Allendoerfer, R. D. *Anal. Chem.* **1976**, *48*, 1446.
(25) Alpoim, M. C.; Urbano, A. M.; Geraldes, C. F. G. C.; Peters, J. A. *J. Chem. Soc., Dalton Trans.* **1992**, 463.
(26) Huskens, J.; Kennedy, A. D.; van Bekkum, H.; Peters, J. *J. Am. Chem. Soc.* **1995**, *117*, 375.
(27) Huskens, J.; Peters, J. A.; van Bekkum, H.; Choppin, G. R. *Inorg. Chem.* **1995**, *34*, 1756.

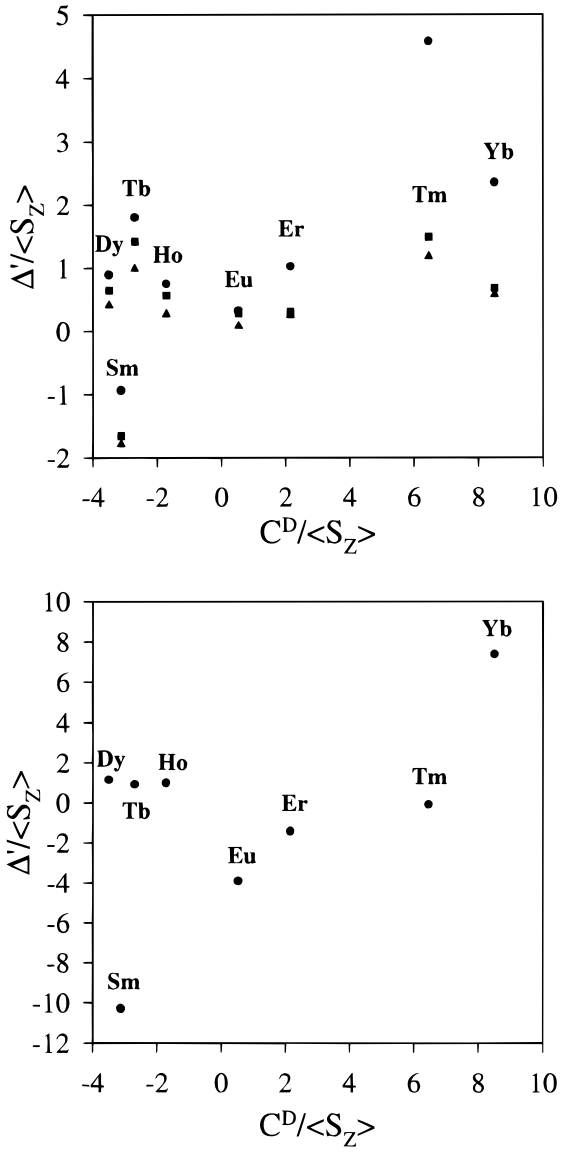

Figure 7. Plot of Δ'/C^D vs $\langle S_Z\rangle/C^D$ for the ^{1}H NMR spectra (See Figure 6 for labeling. Top: ● = hydrogen H_F, ■ = H_G, ▲ = H_H) and for the ^{31}P NMR spectra (bottom) of $[Ln(H_3ppma)_2]^{3+}$ where Ln = Sm−Lu.

dinated to the lanthanide.[26,28] Since the ^{17}O shift is predominantly contact in nature, the slope of a plot of DyIS versus [Dy(III)] should be proportional to the number of bound water molecules associated with the complex. If the hydration number of Dy(III) is taken to be 8,[29] then a slope of −358/8 = −45 would be indicative of one bound water and each multiple of 45 corresponds to one water. Figure 8 shows the DyIS versus [Dy(III)] plots for Dy_{aq}^{3+}, $[Dy(tams)]^{3-}$, and $[Dy(taps)]^{3-}$ (a plot for $[Dy(H_3trns)_2]^{3+}$ [7] is shown for comparison). The slope of −358 ppm/M for Dy_{aq}^{3+} is in excellent agreement with that obtained by Alpoim et al.[25] (−357 ppm/M) and by Reuben and Fiat[30] (−360 ppm/M). The error bars show the line widths at half-height (60 Hz); however, the precision was ±5 Hz. All three plots were linear with correlation coefficients of greater than 0.999. The slopes for $[Dy(tams)]^{3-}$ and $[Dy(taps)]^{3-}$ were −128 ppm/M (2.8 H_2O) and −123 ppm/M (2.7 H_2O), respectively. Ratios of $tams^{6-}$:Dy(III) and $taps^{6-}$:Dy(III) as high as 8 showed a limiting stoichiometry of 1:1 for $tams^{6-}$:Dy(III) and $taps^{6-}$:Dy(III). A study of the hydration of the Dy−H_3ppma system was attempted; however, even at large excesses of ligand, multiple species were present.

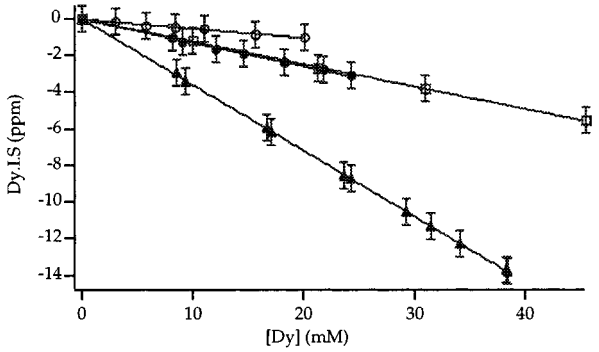

Figure 8. Plot of DyIS vs [Dy(III)] (mM): Dy_{aq}^{3+}, ▲; $[Dy(tams)]^{3-}$, ●; $[Dy(taps)]^{3-}$, □; $[Dy(H_3trns)_2]^{3-}$, ○. Error bars represent line widths at half-height.

Discussion

H_3ppma forms highly (S_6) symmetrical bis(ligand) complexes with the lanthanides Sm−Lu, analogous to those formed with the group 13 metals.[8] Indeed, the X-ray structure of the lutetium complex is isostructural and isomorphous with that of the indium complex. The high symmetry is preserved in solution, indicated in the ^{1}H and ^{31}P NMR spectra. Such evidence indicates an isostructural series of compounds from Sm to Lu. In light of this, it was expected that the paramagnetic shifts of the ^{1}H and ^{31}P resonances could be resolved into contact and pseudocontact components, once corrected for diamagnetic and bulk magnetic susceptibility contributions. However, a linear relationship for Δ'/C^D vs $\langle S_Z\rangle/C^D$ (or $\Delta'/\langle S_Z\rangle$ vs $C^D/\langle S_Z\rangle$) was not forthcoming (Figure 7). Such a failure to correlate strongly suggests a changing coordination geometry or number. In the case of H_3-ppma, all evidence (NMR, mass spectral, IR, and elemental analyses) points toward an isostructural series, especially for Er−Lu. It is evident that subtle changes in ligand orientation about the paramagnetic lanthanide as the ionic radius increases cause sufficiently large changes in chemical shift, to prevent a linear correlation; i.e., the interlocking phenyl groups must move further apart to some extent to accommodate the larger metal ion, even if the change in ionic radius is only small. The opposite of this, i.e., the compression of the phenyl rings, was the rationale for the greater stability of the indium complex with respect to those of gallium and aluminum.[8] Indeed the chemical shifts of the hydrogens ortho to phosphorus in the phenyl rings (H_F) show a progressive shift to lower frequency Al−Ga−In−Lu. The fact that these small changes in geometry cause such a large effect suggests a large pseudocontact contribution to the chemical shift, as it is this contribution which contains structural information. It is stated[17,24,25] that if geometric information for a substrate is to be obtained, the complex must have axial symmetry (at least 3-fold); it is expected that S_6 symmetry here would be more than sufficient.

The bis(ligand) complexes obtained for H_3ppma are similar to those obtained[7] with H_3trns^{3-}, where the oxygen donor group is phenolato as opposed to phosphinato. For complexes of both these ligands, K_1 was found to be less than K_2, an unusual occurrence. In the H_3trns^{3-}−Ln(III) system,[7] it is likely that this unusual phenomenon is predominantly an entropic effect; the nature of the H_3trns^{3-}−Ln(III) system suggests that there

(28) Peters, J. A.; Kieboom, A. P. G. *Recl. Trav. Chim. Pays-Bas* **1983**, *102*, 381.
(29) Helm, L.; Foglia, F.; Kowall, T.; Merbach, A. E. *J. Phys.: Condens. Matter* **1994**, *6*, A137.
(30) Reuben, J.; Fiat, D. *J. Chem. Phys.* **1969**, *51*, 4909.

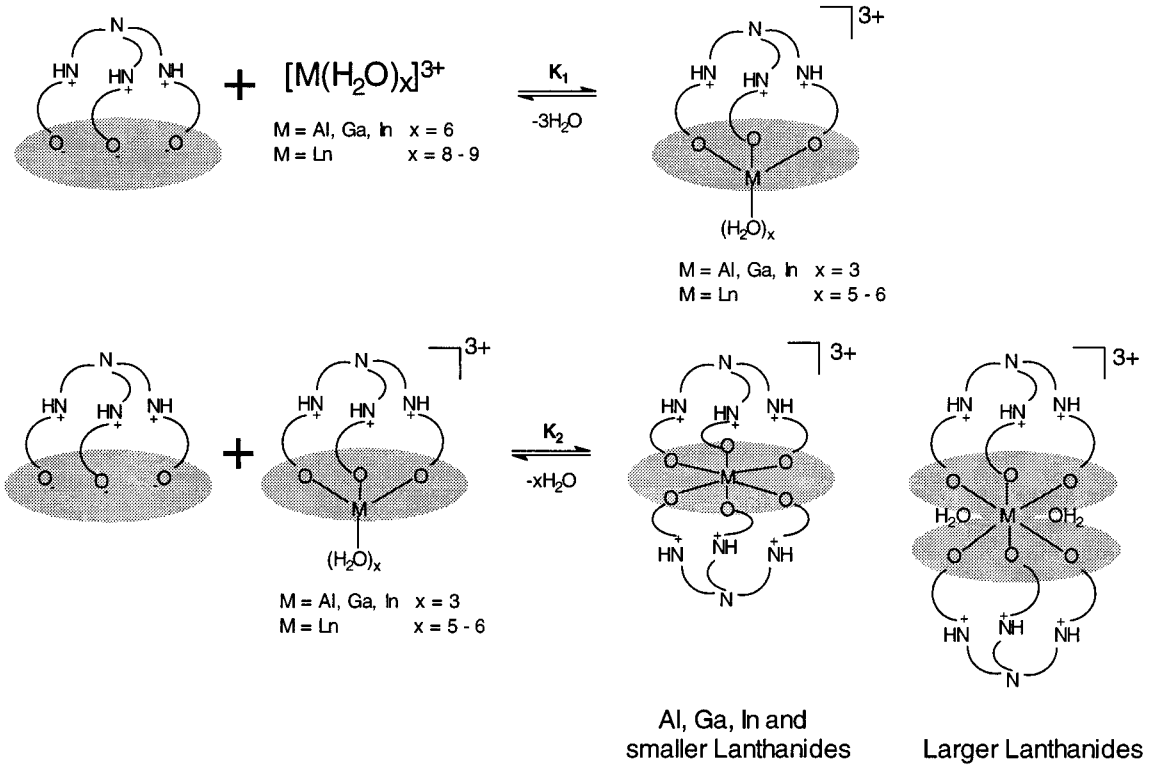

Figure 9. Tightening the hydrophobic belt: the Ln(III)−H_3ppma or −H_3trns^{3-} equilibria viewed in terms of hydrophobic interactions.

should be no favorable enthalpy associated with K_2 (relative to K_1) on the basis of electrostatic arguments and a lowering of coordination number. The first equivalent of H_3trns^{3-} displaced three waters, while the second equivalent displaced five waters; this second equilibrium increased the translational entropy of the system more than the first and was thus manifested in the larger value of K_2. This argument was supported by calorimetric measurements, which showed $S_2 > S_1$ for each Ln(III) studied.[7]

An alternative argument can be proposed for the anomalous $K_2 > K_1$ effect on the basis of the *hydrophobic effect*.[31,32] Consider the solvation of a gaseous hydrocarbon in water at 25 °C. This process involves a small negative enthalpy of solvation but a larger negative entropy of solvation; it is thermodynamically disfavored because of entropy.[32] The aggregation of apolar solutes is then driven by entropy such that the water molecules avoid entropically unfavorable interactions with the apolar solute molecules. H_3trns^{3-} and H_3ppma can be thought of as amphiphilic species with charged polar regions and three apolar aryl rings. Describing the two equilibria, K_1 and K_2, pictorially as in Figure 9 for H_3ppma (the charges differ for H_3trns^{3-}) leads to a hydrophobic interpretation of the two complexation reactions. The areas shaded in gray represent the hydrophobic aryl portions of the molecules.

In the first step (K_1) one ion with a hydrophobic region combines with a lanthanide ion to give a molecule with a hydrophobic region. The second step (K_2) is the combination of a mono(ligand) species with a second ligand, each with a hydrophobic region, combining to give an ion with only one hydrophobic region. This minimization of solvent (H_2O) accessible hydrophobic regions, or "a tightening of the hydrophobic belt", should be reflected in a more positive entropy for K_2 relative to K_1, as was observed for H_3trns^{3-}.[7] Both steps are also enthalpically favored by the formation of Ln−O (phenolate) bonds. This hydrophobic interpretation of the complexation can also be invoked to explain the similar anomalous behavior of the equilibria of the ligand H_3ppma when complexed to the group 13 metals.[8] Topologically the ligand is almost identical to trns^{6-}, having a tripodal tren-based structure bearing pendant donors incorporating a hydrophobic aryl region. H_3ppma reacts with the group 13 metals and with the lanthanides to form capped and bicapped complexes by coordinating to the metal through the phosphinato oxygen atoms. The second stepwise equilibrium constant is markedly greater than the first in the case of the group 13 metals and less so, but still significantly large, in the case of the lanthanides.

Since the aquo ions of Al(III), Ga(III), and In(III) are known to be six-coordinate and the bicapped complexes contain octahedral ions, the argument presented previously for trns^{6-}, i.e., for an inner-sphere desolvation and lowering of coordination number, does not apply. However this anomalous behavior can be rationalized by the hydrophobic effect as shown in Figure 9. In the case of the lanthanides, a reduction of solvation may play a part, but again it is likely that this hydrophobic explanation is applicable. The difference between K_2 and K_1 is not as startling as that for the group 13 metals even though the formation of a six-coordinate lanthanide complex would be expected to exhibit an even greater entropic effect on moving from a monocapped species with the expulsion of five bound waters. The major difference in this case is the increase in size of the coordinated metal ion. H_3ppma showed an increased affinity for the larger metals in group 13, where log K_2 followed the order for In > Ga > Al, increasing by an order of magnitude in each case.[8] The preference for indium was attributed to the ionic radii of the metals, indium being of ideal size to accommodate the bulky phenyl groups on coordination. The determination of the formation constants of the group 13 metals was carried out via a combined ^{31}P−^{27}Al/^{71}Ga NMR spectroscopic method, as the use of more conventional methods

(31) Tanford, C. *The Hydrophobic Effect: Formation of Micelles and Biological Membranes*; John Wiley & Sons: New York, 1973.
(32) Blokzijl, W.; Engberts, J. B. F. N. *Angew. Chem., Int. Ed. Engl.* **1993**, *32*, 1545.

(potentiometry) was obviated by the very low pK_a's of the phosphinic hydroxyls and lack of chromophores (UV/vis). In the case of the lanthanide complexes, the study was restricted to diamagnetic Lu(III) and paramagnetic Yb(III). Attempts with any earlier lanthanides were thwarted by increasing line widths and overlapping of resonances. Even so, a trend is noted, which can be readily explained by considering the "tightening of the hydrophobic belt". Indium, it would appear, is the ideal size to accommodate the six phenyl rings in a strain-free manner, while still excluding solvent from the coordination sphere.[8] The lanthanides show a marked increase in K_1 with respect to the group 13 metals, which can be attributed to their increased ionic radii. The larger the metal ion, the further apart the two ligands become, thus allowing more solvent to be in contact with the hydrophobic areas of the complex (Figure 9); hence the hydrophobic belt is somewhat loosened. This is reflected in the decrease in K_1 relative to K_2 as we move from Yb(III) to Lu(III); indeed it appears that on moving to the larger lanthanides (Ho−Sm), the phenyls will be sufficiently separated to perhaps allow water coordination or at least interference of solvent, causing a breakup of the complexes, as was highlighted by the ^{1}H and ^{31}P NMR spectra of these complexes in CD_3OD. This may also be the cause of the noncorrelation of the lanthanide-induced shift NMR data.

When H_3trns^{3-} binds to a lanthanide(III) in a tridentate fashion, there should be no chelate effect—three 16-membered chelate rings are formed. Given the relatively high stability found for these capped 16-membered ring complexes,[7] there must be an effect which predisposes the ligand to a binding posture. The flexibility imparted by a loose H-bond network coupled with the large chelate ring size results in a tridentate ligand which should have little or no strain energy created in accommodating different Ln(III) ions; thus the increase in stability is purely electrostatic and increases with the inverse ionic radius of the lanthanide considered. To further explore the effect of large chelate ring size on Ln(III) selectivity, solution studies with H_6tams and H_6taps were undertaken. If these two ligands reacted in the same manner as H_6trns, then lanthanide complexes containing 14-membered and 13-membered chelate rings would be formed. Instead of coordinating solely through the phenolato donor atoms, tams^{6-} and taps^{6-} coordinated through the three amino nitrogen and three phenolato oxygen donor atoms. A major difference between H_6trns and H_6tams or H_6taps is the microscopic order of deprotonation. It had been shown that the first three deprotonation events of H_6trns occur at phenolic sites,[7] whereas H_6tams and H_6taps are first deprotonated at an ammonium site, followed by three phenol sites, and then the remaining two ammonium groups.[6] The first deprotonation of H_6tams and H_6taps occurs at a pH much lower than that at which Ln(III) complexation occurs. Hence coordination to this amino group should be facile. Coordination to one amino group would necessarily bring the remaining ammonium groups closer to the metal ion to allow for proton displacement and lanthanide coordination to give the observed N_3O_3 ligand donor set. Variation of the donor group in changing from H_3trns^{3-} to H_3ppma, i.e., from phenolato to phosphinato, showed no dramatic change in coordination as shown for tams^{6-} and taps^{6-}. Indeed, none is expected as both ligands have nitrogen pK_a's which are higher than the oxygen pK_a's, the much lower phenolato and phosphinato pK_a's dictate binding to the lanthanides exclusively through oxygen.

The ^{17}O NMR study of both [Dy(tams)]$^{3-}$ and [Dy(taps)]$^{3-}$ (Figure 8) indicated the presence of three inner-sphere water molecules, implying a nine-coordinate Dy(III) in each of the

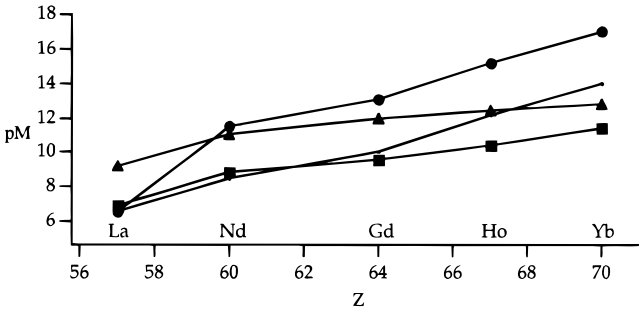

Figure 10. Comparative pM values vs Z: H_3trns^{3-}, [Ln(III)]$_{tot}$ = 1 mM, ●; H_3trns^{3-}, [Ln(III)]$_{tot}$ = 1 μM, line; taps^{6-}, [Ln(III)]$_{tot}$ = 1 mM, ▲; tams^{6-}, [Ln(III)]$_{tot}$ = 1 mM, ■.

complexes. The change in coordination mode from H_3trns^{3-} to tams^{6-} and taps^{6-} has a profound effect on the metal ion selectivity. There is a large increase in stability upon going from La(III) to Nd(III) for all three ligands. However, on going from Nd(III) to Yb(III), H_3trns^{3-} exhibited a selectivity of about 2 log units per lanthanide studied. Here tams^{6-} exhibits lesser selectivity, about 1 log unit per lanthanide studied, whereas taps^{6-} has a much lower selectivity between Gd(III) and Yb(III). A better way of analyzing the data is to take into account the competition with the hydrogen ion for the ligand by calculating pM values where pM = −log [M$_{free}$]. This gives an impression of the relative sequestering ability of the ligands under a standard set of conditions. In Figure 10, pM values are calculated at pH 7.4 for a ligand-to-metal ratio of 10:1. The total concentration of Ln(III) is set at 1 mM; however since the stability constants for H_3trns^{3-} have an inverse square dependence on [H_3trns^{3-}], the pM values for [Ln]$_{tot}$ = 1 μM have also been calculated to highlight this dilution effect. At millimolar concentrations and above, H_3trns^{3-} is the best ligand for complexing Nd(III) → Yb(III), and its sequestering ability increases with atomic number, Z. The much flatter curve for taps^{6-} indicates that it is less able to discriminate between the lanthanides.

The major structural difference between taps^{6-} and tams^{6-} is that taps^{6-} coordinates to a lanthanide forming four six- and two five-membered chelate rings, whereas tams^{6-} forms only six-membered chelate rings upon coordination. An established tenet of coordination chemistry is that five-membered chelate rings are more stable than six-membered chelate rings and this difference in stability increases with increasing metal ion size.[33] This effect is manifested here where [Ln(taps)]$^{3-}$ complexes are 1−2 orders of magnitude more stable than the analogous [Ln(tams)]$^{3-}$ complexes.

Concluding Remarks

The ligand H_3ppma has been shown to form S_6-symmetric bicapped bis(ligand) complexes with the lanthanides (as seen in the X-ray crystal structure of the lutetium complex, and in solution NMR studies), whereby it binds as a tridentate ligand exclusively via the phosphinato groups. These complexes are isostructural with those obtained with the group 13 metals[8] and similar to those obtained when the oxygen donor is phenolato.[7] However, moving to the slightly smaller tripodal amines with phenolate donors, tams^{6-} and taps^{6-}, coordination to lanthanides in a hexadentate fashion is observed through three amino nitrogens and three phenolato oxygen donors. The ability of these aminephenolates to coordinate through the amino group

(33) Hancock, R. D.; Martell, A. E. *Chem. Rev.* **1989**, *89*, 1875.

is a consequence of the low pK_a of one of the ammonium moieties in these compounds. The selectivity for the late lanthanides by $taps^{6-}$ and $tams^{6-}$ is considerably muted compared to that of H_3trns^{3-}. ^{17}O NMR established that the coordination number for $[Dy(tams)(H_2O)_3]^{3-}$ is 9 (N_3O_6) and that for $[Dy(taps)(H_2O)_3]^{3-}$ is 9 (N_3O_6).

Acknowledgment is made to the Natural Sciences and Engineering Research Council (NSERC) for a postgraduate scholarship to P.C. (1992−6), to the NSERC and Du Pont Merck Pharmaceutical Co. for operating funds, to Professor J. Trotter for the very kind use of his crystallographic facilities, and Ms. Parisa Mehrkhodavandi for experimental assistance.

Supporting Information Available: Complete tables of crystallographic data, final atomic coordinates and equivalent isotropic thermal parameters, anisotropic thermal parameters, bond lengths, bond angles, torsion angles, intermolecular contacts and least-squares planes, as well as tables of infrared and mass spectral data and an ORTEP diagram (14 pages). Ordering information is given on any current masthead page.

IC971488G